ChemComm

COMMUNICATION

View Article Online
View Journal | View Issue

Cite this: *Chem. Commun.*, 2025, **61**, 15842

Received 30th May 2025,
Accepted 4th September 2025

DOI: 10.1039/d5cc03046c

rsc.li/chemcomm

The relative importance of contact-angle hysteresis and work of adhesion on droplet "roll-off" or sliding angles

Fatema B. Amin [a] and Gregory S. Ferguson *[ab]

A series of mixed monolayers formed by self-assembly of alkanethiols on gold exhibits complementary wetting behavior for hexadecane and water that allowed us to independently assess how strongly the contact-angle hysteresis and work of adhesion of contacting liquid droplets influence their sliding angles on these surfaces. Near-constant values of advancing contact angle, and thus work of adhesion, for droplets of water across this series enabled the study of the relationship between the contact-angle hysteresis and the sliding angle. The same surfaces exhibited near-constant hysteresis, but varying values of work of adhesion, with hexadecane as the wetting liquid. These complementary studies confirmed a correlation between droplet sliding angle and hysteresis, with the work of adhesion playing little or no role.

The tilt angle of a planar substrate at which a droplet of liquid begins to move is known as the "roll-off" or "sliding" angle. The forces that govern this property have been the subject of a long history of theoretical study, culminating in an increasingly detailed description,[1–9] and Tadmor has recently provided a review of developments in this area.[10] The macroscopic mechanics described in these descriptions are a balance of opposing forces, the component of gravitation directed along the downward tilt, and the drag introduced by pinning at the leading and trailing edges of the drop. Throughout the iterations of development, the magnitude of the latter force ($f_{\parallel}$)—static friction prior to droplet motion—is treated as proportional to the hysteresis in the contact angle at the two drop edges ($\cos\theta_r - \cos\theta_a$), which provides a macroscopic measure of the collective effect of local molecular-level pinning (eqn (1)).[10,11] These treatments have indicated no influence of the work of adhesion (W_{ad}), expressed here as the idealized Young–Dupré equation (eqn (2)),[12]

$$f_{\parallel} \propto (\cos\theta_r - \cos\theta_a) \quad (1)$$

$$W_{ad} = \gamma_{lv}(1 + \cos\theta_a) \quad (2)$$

where γ_{lv} represents the interfacial tension at the liquid–vapor boundary. Nonetheless, suggestions to the contrary have appeared in the literature, and the current study is intended to provide some experimental clarity on the issue.

The development of a theoretical framework for understanding sliding angles has been accompanied by extensive research on the use of engineered surfaces to enhance performance by tuning sliding angles, for example, in microfluidics,[13] food packaging,[14] biomedical,[15] electronic devices with fluid-repellent surfaces,[16] self-cleaning,[17] and anti-icing.[18] Several studies have linked droplet sliding or pinning events to the contact-angle hysteresis,[19] local defects,[20] and the forces acting on a droplet when placed on a tilted surface.[10,21]

In our previous paper investigating a series of single-component self-assembled monolayers (SAMs) on silicon,[22] we found that the sliding angle of hexadecane had little or no dependence on the work of adhesion (eqn (2)) for substrates with approximately the same contact-angle hysteresis. In the current publication, we expand and extend those studies with a series of two-component SAMs on gold that allow us to independently assess both the influence of the contact-angle hysteresis and the work of adhesion by using two different droplet liquids. We have used one polar and one purely dispersive liquid, water and hexadecane, and leveraged their complementary wetting behaviors on mixed monolayers to address these questions systematically.

In early studies, Bain and Whitesides found that SAMs adsorbed from ethanol solutions containing mixtures of two *n*-alkanethiols of different lengths displayed uniquely different wetting behavior with water and hexadecane.[23,24] In particular, the advancing contact angles of water (and hence W_{ad}) on mixed SAMs adsorbed from solutions containing $CH_3(CH_2)_{11}SH$ and $CH_3(CH_2)_{21}SH$ were relatively insensitive to the concentrations of the two components, whereas the hysteresis in the contact angle varied significantly. The wetting behavior was reversed for hexadecane: the hysteresis in the contact angle was relatively

[a] *Department of Chemistry, Lehigh University, Bethlehem, PA 18015, USA. E-mail: gf03@lehigh.edu*
[b] *Department of Materials Science and Engineering, Lehigh University, Bethlehem, PA 18015, USA*

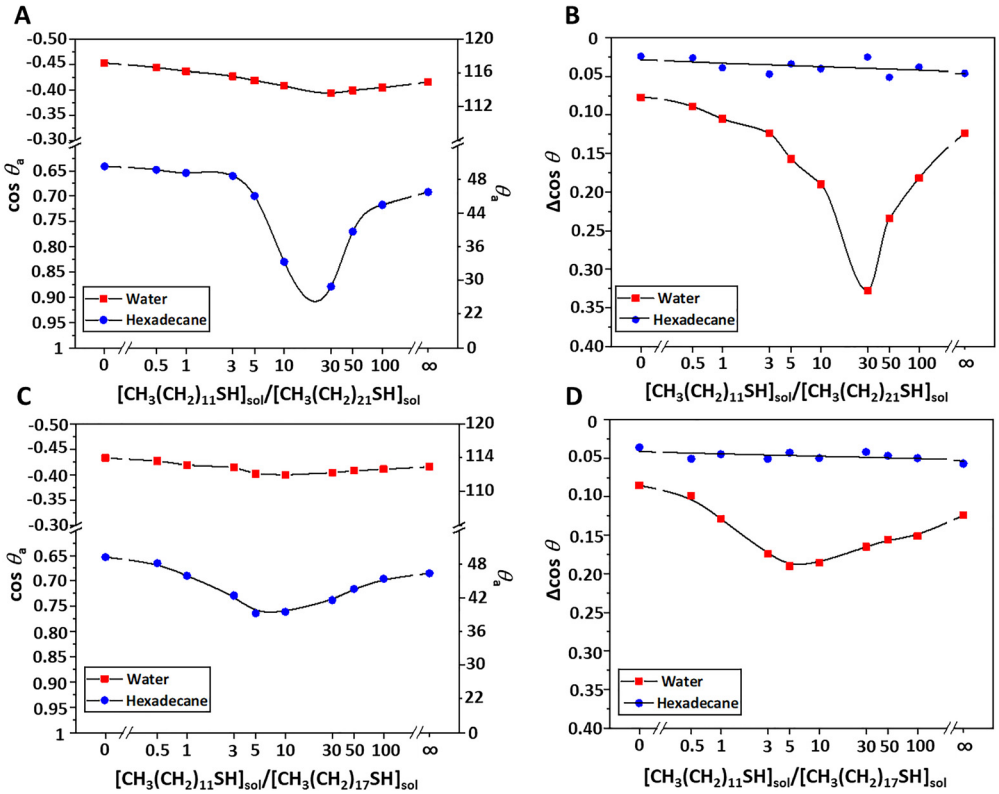

Fig. 1 Advancing contact angles ($\cos\theta_a$, and θ_a) and contact-angle hysteresis for water (red) and hexadecane (blue) as a function of the ratio of adsorbate concentrations in solutions used to form the substrate monolayers. (A) and (B) $[CH_3(CH_2)_{11}SH]_{sol}/[CH_3(CH_2)_{21}SH]_{sol}$. (C) and (D) $[CH_3(CH_2)_{11}SH]_{sol}/[CH_3(CH_2)_{17}SH]_{sol}$. The *x*-coordinates in all figures are plotted on a logarithmic scale, and the lines connecting data points are simply guides for the eye.

insensitive to the adsorbate composition, whereas the advancing contact angles varied significantly. The authors suggested that this behavior may reflect differences in interfacial entropy at interfaces between these liquids and the disordered surfaces of the mixed hydrocarbon monolayers. These properties were ideally suited to enable our current study of sliding angle, by allowing us to measure the effects of two potential variables—contact-angle hysteresis and advancing contact angle (and thus the Young–Dupré work of adhesion)—independently. Our studies focused on SAMs formed from $CH_3(CH_2)_{11}SH$/$CH_3(CH_2)_{21}SH$ solution mixtures, as well as those from analogous $CH_3(CH_2)_{11}SH$/$CH_3(CH_2)_{17}SH$ mixtures for comparison. We examined the wetting and droplet-sliding behavior on SAMs adsorbed from solutions with molar ratios, $[CH_3(CH_2)_{11}SH]$/$[CH_3(CH_2)_nSH]$, of 0, 0.5, 1, 3, 5, 10, 30, 50, 100, and infinity (pure $CH_3(CH_2)_{11}SH$), where *n* equals 17 or 21. Our SAMs were prepared under slightly different conditions from ref. 24, as described in the SI.

The wettability measurements, shown graphically in Fig. 1 for both types of mixed SAM, are generally consistent with the literature values.[23,24] The advancing contact angle of water (θ_a or $\cos\theta_a$) remained almost constant, to within 4°, over the range of composition for both sets of mixed monolayer (Fig. 1A and C). The hysteresis ($\Delta\cos\theta$, *i.e.*, $\cos\theta_r - \cos\theta_a$) in the contact angle of water, however, showed a pronounced dependence on composition (Fig. 1B and D). The contrasting wetting behavior of hexadecane on these surfaces also confirmed the earlier results for mixed SAMs adsorbed from $CH_3(CH_2)_{11}SH$ and $CH_3(CH_2)_{21}SH$.[24] The advancing contact angle of hexadecane varied significantly over the composition range, with maximum values for the pure monolayers and a minimum value between solution ratios of 10 and 30. In contrast, the hysteresis in the contact angle of hexadecane on these surfaces was insensitive to composition. Decreasing the difference in chain length between two thiols generally muted the variations in the advancing contact angle of water and hysteresis of hexadecane, as a function of the ratio of adsorbate solution concentrations. The extrema in the plots in Fig. 1 are also shifted toward lower adsorbate ratios for the samples with a smaller difference in chain length. For example, the hysteresis was higher for the mixed SAMs than for the pure SAMs and was largest for a solution ratio of 30 for the $CH_3(CH_2)_{11}SH$/$CH_3(CH_2)_{21}SH$ system and between 5–10 for the $CH_3(CH_2)_{11}SH$/$CH_3(CH_2)_{17}SH$ system.

The sliding angles for liquid droplets on these surfaces were determined by placing a ~10 μL droplet from a blunt-tipped needle onto a horizontal surface and slowly inclining the stage in 1° increments until the onset of droplet motion. The needle was positioned just above the surface to minimize the kinetic energy imparted to the droplet. The onset, or lack, of motion along the inclined surface was tracked visually in real time using a CCD camera with a software interface. A consistent droplet volume was used for all the measurements to minimize

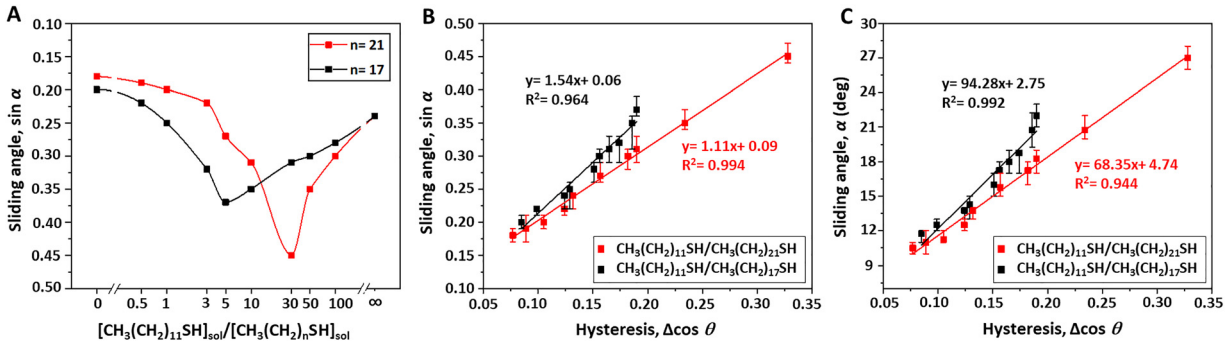

Fig. 2 Sliding angles (sin α and α) of water as a function of: (A) the ratio of solution adsorbate concentrations, $[CH_3(CH_2)_{11}SH]_{sol}/[CH_3(CH_2)_nSH]_{sol}$, where n = 21 (red) or 17 (black); and (B) and (C) the contact-angle hysteresis (Δcos θ) on monolayers adsorbed from mixtures of $CH_3(CH_2)_{11}SH$ and $CH_3(CH_2)_{21}SH$, or of $CH_3(CH_2)_{11}SH$ and $CH_3(CH_2)_{17}SH$. The lines connecting the data points in 2A serve as visual aids. Error bars in 2B and 2C indicate the maximum–minimum range of sliding angle measurements for four droplets per sample.

any influences related to differences in gravitational force and droplet size.

The near-constant advancing contact angle (and thus Young–Dupré work of adhesion) of water as a function of composition, across both sets of mixed SAMs (Fig. 1A and C), enabled us to isolate the dependence of the sliding angle of water droplets on contact-angle hysteresis alone. Fig. 2 shows the sine of the sliding angle for water droplets over the range of SAM composition (Fig. 2A) and as a function of the corresponding contact-angle hysteresis (Δcos θ, Fig. 2B) for both sets of mixed SAMs. The values of sin α are used rather than α itself because sin α is directly proportional to the frictional force opposing droplet motion ($f_{\parallel}$, eqn (1)).[10] For comparison, plots of the sliding angles (α) directly are provided in Fig. 2C; the similarities reflect the near linearity of the sine function with the angles in this range. The shapes of the plots in Fig. 1B and 2A (red, n = 21) are strikingly similar, consistent with the expected linear relationship between sin α and Δcos θ, with both plots reaching a maximum value of the dependent variable at a molar solution ratio of 30 ($CH_3(CH_2)_{11}SH/CH_3(CH_2)_{21}SH$). The full range of sin α was 0.16–0.45 (α, 10–27°; Fig. 2C). The linear relationship between sin α and Δcos θ is confirmed in the direct plot in Fig. 2B. The system with a smaller difference in alkyl-chain length, $CH_3(CH_2)_{11}SH/[CH_3(CH_2)_{17}SH$, showed analogous similarities between Fig. 1D and 2A (black, n = 17), with less pronounced changes relative to the other system, as expected. The full range of sin α in this case was 0.20–0.37 (α, 12–22°; Fig. 2C). The linear relationship between sin α and Δcos θ is confirmed in this case as well, over the smaller change in Δcos θ.

In contrast to the behavior of water on these surfaces, hexadecane exhibited a dramatic decrease in advancing contact angle for the mixed SAMs, falling by almost half from the value found for a pure $C_{22}H_{45}SH$ monolayer in the $CH_3(CH_2)_{11}SH/CH_3(CH_2)_{21}SH$ system (Fig. 1A). The drop in advancing angle is much more modest in Fig. 1C for the mixed SAMs with a smaller difference in chain lengths ($CH_3(CH_2)_{11}SH/CH_3(CH_2)_{17}SH$). The hysteresis in the contact angle of hexadecane, however, is nearly constant with only a 2°–3° variation across the range of composition (Fig. 1B and D). This nearly constant hysteresis effectively removes it as a variable and allows us to assess the dependence of sliding angles on the advancing contact angle, and hence on the work of adhesion (eqn (2)) for the same set of samples. The sliding angle, measured with four different droplets of hexadecane on each type of

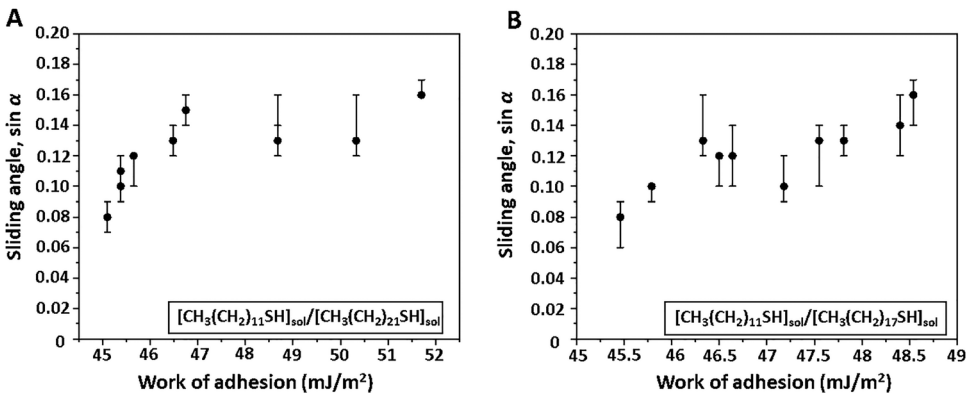

Fig. 3 Sine of sliding angles (sin α) of hexadecane is plotted against the work of adhesion on mixed monolayers. (A) $[CH_3(CH_2)_{11}SH]_{sol}$ and $[CH_3(CH_2)_{21}SH]_{sol}$. (B) $[CH_3(CH_2)_{11}SH]_{sol}$ and $[CH_3(CH_2)_{17}SH]_{sol}$. Error bars represent the maximum–minimum range of sliding angle measurements on four droplets per sample.

mixed monolayer, shows little or no discernible correlation with the work of adhesion (assuming a surface tension of 27.5 mJ m^{-2} for hexadecane) across the range of ~45–52 mJ m^{-2} in either set of thiol mixture (Fig. 3).

In summary, we have examined the sliding angles of droplets of a polar liquid (water) and of a non-polar liquid (hexadecane) on the same mixed SAMs on gold, prepared by adsorption from solutions containing binary mixtures of different alkanethiols. The wetting behavior—advancing contact angle (and thus work of adhesion) and hysteresis in the contact angle—of these two liquids differed in a complementary way across the range of relative concentrations used to prepare the mixed SAMs. This complementarity allowed us to independently study the importance of these variables in determining droplet sliding angles on a common set of surfaces. We found a strong dependence of the sliding angle on contact-angle hysteresis, but little or no dependence on the work of adhesion. Both results are consistent with current theoretical predictions and older semi-empirical descriptions.

Conflicts of interest

There are no conflicts to declare.

Data availability

The experimental procedure and data supporting this article have been included in the SI. See DOI: https://doi.org/10.1039/d5cc03046c

Acknowledgements

Funding for the purchase of a spectroscopic ellipsometer was provided by a grant from the National Science Foundation (CHE-0923370). This article is dedicated to Professor George M. Whitesides, as part of the themed collection celebrating his 85th birthday.

Notes and references

1 Y. Yonemoto, S. Suzuki, S. Uenomachi and T. Kunugi, Sliding Behaviour of Water-Ethanol Mixture Droplets on Inclined Low-Surface-Energy Solid, *Int. J. Heat Mass Transfer*, 2018, **120**, 1315–1324.
2 M. Sakai, J.-H. Song, N. Yoshida, S. Suzuki, Y. Kameshima and A. Nakajima, Relationship between Sliding Acceleration of Water Droplets and Dynamic Contact Angles on Hydrophobic Surfaces, *Surf. Sci.*, 2006, **600**(16), L204–L208.
3 G. Ahmed, M. Sellier, M. Jermy and M. Taylor, Modeling the Effects of Contact Angle Hysteresis on the Sliding of Droplets down Inclined Surfaces, *Eur. J. Mech.*, 2014, **48**, 218–230.
4 W. Y. L. Ling, T. W. Ng, A. Neild and Q. Zheng, Sliding Variability of Droplets on a Hydrophobic Incline Due to Surface Entrained Air Bubbles, *J. Colloid Interface Sci.*, 2011, **354**(2), 832–842.
5 Y. Ding, L. Jia, Q. Peng and J. Guo, Critical Sliding Angle of Water Droplet on Parallel Hydrophobic Grooved Surface, *Colloids Surf., A*, 2020, **585**, 124083.
6 J. J. Bikerman, Sliding of Drops from Surfaces of Different Roughnesses, *J. Colloid Sci.*, 1950, **5**(4), 349–359.
7 J. J. Bikerman, Surface Roughness and Sliding Friction, *Rev. Mod. Phys.*, 1944, **16**(1), 53.
8 L. Mahadevan and Y. Pomeau, Rolling Droplets, *Phys. Fluids*, 1999, **11**(9), 2449–2453.
9 C. Huh and L. E. Scriven, Hydrodynamic Model of Steady Movement of a Solid/Liquid/Fluid Contact Line, *J. Colloid Interface Sci.*, 1971, **35**(1), 85–101.
10 R. Tadmor, Open Problems in Wetting Phenomena: Pinning Retention Forces, *Langmuir*, 2021, **37**(21), 6357–6372.
11 Y. Di, J. Qiu, G. Wang, H. Wang, L. Lan and B. Zheng, Exploring Contact Angle Hysteresis Behavior of Droplets on the Surface Microstructure, *Langmuir*, 2021, **37**(23), 7078–7086.
12 More recent studies suggest that the work of adhesion should be expressed as a function of the (cosine of the) receding angle or average of the advancing and receding angles. On an ideal surface, with zero hysteresis, these values would all be the same. (*a*) D. L. Schmidt, R. F. Brady, K. Lam, D. C. Schmidt and M. K. Chaudhury, Contact Angle Hysteresis, Adhesion, and Marine Biofouling, *Langmuir*, 2004, **20**(7), 2830–2836; (*b*) G. McHale, G. G. Wells and R. Ledesma-Aguilar, Surfaces Slippery to Liquids: Wettability, Adhesion, and Contact Line Friction, *Langmuir*, 2025, **41**(23), 14579–14588.
13 S. Ling, Y. Luo, L. Luan, Z. Wang and T. Wu, Inkjet Printing of Patterned Ultra-Slippery Surfaces for Planar Droplet Manipulation, *Sens. Actuators, B*, 2016, **235**, 732–738.
14 M. Ruzi, N. Celik and M. S. Onses, Superhydrophobic Coatings for Food Packaging Applications: A Review. Food Packag. Shelf, *Life*, 2022, **32**, 100823.
15 X. Wang, Z. Zhuang, X. Li and X. Yao, Droplet Manipulation on Bioinspired Slippery Surfaces: From Design Principle to Biomedical Applications, *Small Methods*, 2023, 2300253.
16 J. E. Mates, I. S. Bayer, J. M. Palumbo, P. J. Carroll and C. M. Megaridis, Extremely Stretchable and Conductive Water-Repellent Coatings for Low-Cost Ultra-Flexible Electronics, *Nat. Commun.*, 2015, **6**(1), 8874.
17 S. S. Latthe, R. S. Sutar, V. S. Kodag, A. K. Bhosale, A. M. Kumar, K. K. Sadasivuni, R. Xing and S. Liu, Self–Cleaning Superhydrophobic Coatings: Potential Industrial Applications, *Prog. Org. Coat.*, 2019, **128**, 52–58.
18 K. Zhang, J. Li, Y. Wang, C. Lin, J. Zhao, Y. Liu and S. Chen, Anti-Icing of Solid Surfaces Based on Droplet Dynamics, *Mod. Phys. Lett. B*, 2023, 2330002.
19 A. Marmur, Contact-Angle Hysteresis on Heterogeneous Smooth Surfaces: Theoretical Comparison of the Captive Bubble and Drop Methods, *Colloids Surf., A*, 1998, **136**(1–2), 209–215.
20 J. F. Joanny and P.-G. De Gennes, A Model for Contact Angle Hysteresis, *J. Chem. Phys.*, 1984, **81**(1), 552–562.
21 E. L. Decker and S. Garoff, Contact Line Structure and Dynamics on Surfaces with Contact Angle Hysteresis, *Langmuir*, 1997, **13**(23), 6321–6332.
22 K. Khadka and G. S. Ferguson, Does the Roll-off Angle Depend on Work of Adhesion?, *Langmuir*, 2022, **38**(16), 4820–4825.
23 C. D. Bain, E. B. Troughton, Y. T. Tao, J. Evall, G. M. Whitesides and R. G. Nuzzo, Formation of Monolayer Films by the Spontaneous Assembly of Organic Thiols from Solution onto Gold, *J. Am. Chem. Soc.*, 1989, **111**(1), 321–335.
24 C. D. Bain and G. M. Whitesides, Formation of Monolayers by the Coadsorption of Thiols on Gold: Variation in the Length of the Alkyl Chain, *J. Am. Chem. Soc.*, 1989, **111**(18), 7164–7175.